

Available online at [www.sciencedirect.com](http://www.sciencedirect.com)**ScienceDirect**

Procedia Structural Integrity 1 (2016) 098–105

Structural Integrity

**Procedia**[www.elsevier.com/locate/procedia](http://www.elsevier.com/locate/procedia)

XV Portuguese Conference on Fracture, PCF 2016, 10-12 February 2016, Paço de Arcos, Portugal

## Numerical study of fatigue crack initiation and propagation on optimally designed cruciform specimens

R. Baptista<sup>a,b,\*</sup>, R. A. Cláudio<sup>a,b</sup>, L. Reis<sup>b</sup>, J. F. A. Madeira<sup>b,c</sup>, M. Freitas<sup>b</sup><sup>a</sup> ESTSetúbal, Instituto Politécnico De Setúbal, Campus do IPS, Estefanilha, 2910-761 Setúbal, Portugal.<sup>b</sup> IDMEC, Instituto Superior Técnico, Universidade de Lisboa, Av. Rovisco Pais, 1049-001 Lisboa, Portugal.<sup>c</sup> ISEL, Instituto Superior de Engenharia de Lisboa, Rua Conselheiro Emídio Navarro, 1,1959-007 Lisboa, Portugal

### Abstract

A new generation of smaller and more efficient biaxial fatigue testing machines has arrived on the market. Using electrical motors these machines are not able to achieve the higher loads their hydraulic counterparts can, and therefore the cruciform specimen needs to be optimized. Following the authors previous work, several different optimal specimens' configurations were produced, using the base material sheet thickness as the main design variable. Every design variable was optimized in order to produce the highest stress level on the specimen center, while the stress distribution is still uniform on a 1 mm radius of the specimen center. Also it was guaranteed that the stress level on the specimen arms was always considerably lower, in order to achieve failure at the specimen center. In this paper traditional criteria like Findley, Brown-Miller, Fatemi-Socie, Smith, Watson e Topper (SWT), Liu I and Chu were considered to determine crack initiation direction for several loads in this biaxial in-plane specimens. In order to understand the fatigue propagation behavior, the stress intensity factors for mode I and mode II was determined for different cracks introduced on the geometry. Several crack and loading parameters were studied, including the starting crack length and angle, and different loading paths. Several biaxial loads were applied to the model, including 30°, 45°, 60°, 90° and 180° out-of-phase angles.

Copyright © 2015 The Authors. Published by Elsevier B.V. This is an open access article under the CC BY-NC-ND license (<http://creativecommons.org/licenses/by-nc-nd/4.0/>).

Peer-review under responsibility of the Scientific Committee of PCF 2016.

**Keywords:** Fracture, Fatigue, In-phase, Out-of-phase, Biaxial, Cruciform.

\* Corresponding author. Tel.: +351 265 790 000; fax: +351 265 790 043.  
E-mail address: [ricardo.baptista@estsetubal.ips.pt](mailto:ricardo.baptista@estsetubal.ips.pt)

## 1. Introduction

The understanding of biaxial fatigue behavior of materials is very important. Especially when considering out-of-phase loading effects, as Cláudio et al. (2014) have demonstrated. As time passes the price of testing equipment tend to decrease and new and more efficient machines are available, in order to test different and more complex loading cases. Freitas et al. (2013) have developed a new testing machine, capable of applying complex biaxial loading paths, closer to the ones applied to automotive and aeronautical structures. Unfortunately the maximum loading capabilities of these machines tend to be more limited, and an optimization of the test specimens has to be pursued in order to obtain high stress levels on the specimen using lower loads. R. Baptista et al. (2015) have developed optimal geometries for different specimen thickness commercially available. These specimens were developed considering the optimal fatigue crack initiation conditions, high stress levels on the specimen center and uniform strain distribution, but how will they behave once the crack as initiated the fatigue propagation process?

In this paper the author set out to answer this question, and to determine the influence of out-of-phase loading on the fatigue behavior. To achieve this goal one must firstly determine the initial crack initiation direction, and secondly determine the fatigue crack propagation direction, as a function of out-of-phase loading. Claudio et al. (2014) and Babaei et al. (2015), have demonstrated that critical plane parameters, like SWT or Fatemi-Socie and many others are ready to be applied to estimate crack initiation direction, unfortunately several material parameters must be experimentally determined. These authors have used out-of-phase loading paths, with loading phase differences to study the material fatigue behaviors, but Misak et al. (2013) has also used more complex loading paths, as star paths and other examples. Once the crack has initiated the crack propagation problem is more complex due to the fact that there are two loads in different directions applied to the specimen. Therefore an equivalent parameter must be used to take into account both crack opening modes. Gotoh et al. (2015) have simulated using finite elements the crack propagation, under non-proportional conditions, of a simple crack normal to the principal loading direction. Misak et al. (2014), (2013) have also studied the influence of non-proportional loading path using the J integral parameter to determine the fatigue crack propagation life of the specimens. Plank et al. (1999) and Singh et al. (1987) have also studied the influence of non-proportional loading on the fatigue crack propagation direction using different approaches. A review of different methods has been done by Zerres et al. (2014), allowing the development of this paper.

## 2. Material and Methods

### 2.1. Cruciform Specimen Design

R. Baptista et al. (2015) have developed the specimens that were studied in this paper. The specimen is based on a cruciform configuration, Fig. 1, and eleven optimal configurations were obtained, considering the Renard Series of preferred numbers one configuration was optimized for each sheet thickness available from 1 to 10 mm. The results presented in this paper are focused on the 2 mm thickness specimen, but can be reproduced for any configuration. The specimens were developed for fatigue crack initiation studies, therefore feature a corner elliptical fillet between the specimen arms, in order to reduce the stress concentration, and to obtain higher stress level on the specimen center. The specimen also features a reduced center thickness, using a revolved spline that increases the stress level on the specimen center and increases the strain distribution uniformity, allowing for the necessary conditions for the fatigue crack initiation to occur on the specimen center.

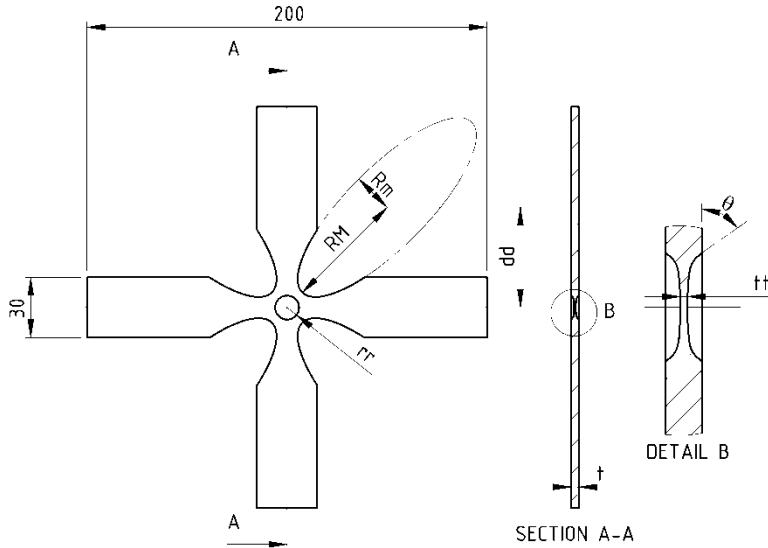


Fig. 1. Cruciform Specimen.

## 2.2. Loading

Biaxial in-plane fatigue loading is characterized by two different loads ( $F_1$  and  $F_2$ ) applied to each of the specimen arms. The loads are applied in perpendicular directions and therefore will be the two main loading directions. Considering that the specimen thickness is small, the material will be subjected to plane stress conditions, and therefore the specimen arms are also the principal directions of the resulting stress distribution and in this case loading is always proportional, Socie and Marquis (2000).

The load cases presented above in this work are unitary, according to eq. (1) where  $\delta$  is the phase shift.

$$F_1 = \sin(t); F_2 = \sin(t + \delta) \quad (1)$$

The applied loads can then be in-phase (fig. 2 a)) when  $\delta=0$ , becoming the relation between  $F_1$  and  $F_2$  constant. In order to introduce an out-of-phase loading path, one can simply introduce a phase shift between the loads. Fig. 2 c) represents a  $30^\circ$  shift and the load ratio is no longer constant, with the load path being represented by an ellipse. Fig. 2 d) and e) show the applied loads for a  $45^\circ$  and  $60^\circ$  phase shift. When the phase reaches  $90^\circ$  the loading path is represented by a circle, Fig. 2 f). And when the load is fully reversed, Fig. 2 b), the phase angle is  $180^\circ$  and  $F_1$  and  $F_2$  have always different signs.

## 2.3. Fatigue Crack Initiation

In order to study the fatigue crack propagation as a function the out-of-phase loading paths, one must determine the fatigue crack initiation direction. This is a necessary step, as the considered specimens do not feature crack initiation notch and the direction of the initial crack is not known.

Therefore it is necessary to consider critical plane models to determine the plane, and therefore the direction, where the crack will initiate. In this paper several criteria were considered, including the Findley (1), Brown-Miller parameter (3), the Fatemi-Socie parameter (4), Smith, Watson e Topper (SWT) (5), Liu I parameter (6) and the Chu (7).

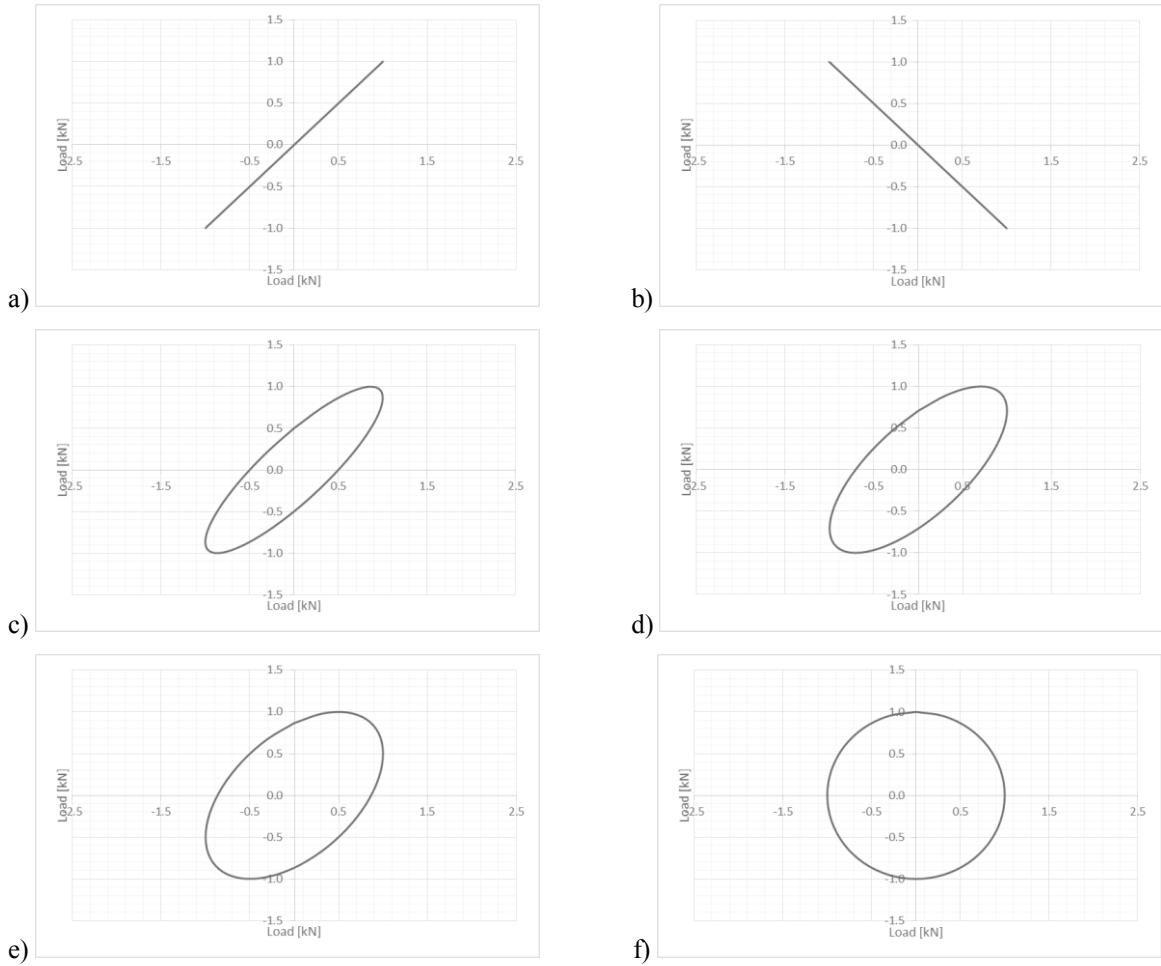


Fig. 2. In-phase and out-of-phase loading applied. a) In-Phase loading, b) Phase angle 180°, c) Phase angle 30°, d) Phase angle 45°, e) Phase angle 60°, f) Phase angle 90°

$$\max_{\beta}(\tau_{\alpha} + k\sigma_{n,max}) \tag{2}$$

$$\max_{\beta}\left(\frac{\Delta\gamma_{max}}{2} + S\Delta\varepsilon_n\right) \tag{3}$$

$$\max_{\beta}\left(\frac{\Delta\gamma_{max}}{2}\left(1 + k\frac{\sigma_{n,max}}{\sigma_y}\right)\right) \tag{4}$$

$$\max_{\beta}\left(\sigma_n\frac{\Delta\varepsilon_1}{2}\right) \tag{5}$$

$$\Delta W = (\Delta\sigma_n\Delta\varepsilon_n)_{max} + (\Delta\tau\Delta\gamma) \tag{6}$$

$$\Delta W = \left(\tau_{n,max}\frac{\Delta\gamma}{2} + \sigma_{n,max}\frac{\Delta\varepsilon}{2}\right) \tag{7}$$

Where  $\sigma$  is the normal stress,  $\varepsilon$  the normal strain,  $\tau$  the shear stress,  $\gamma$  the shear strain, and  $S$  and  $k$  are material parameters. The maximum are in a specific plane with a  $\beta$  angle.

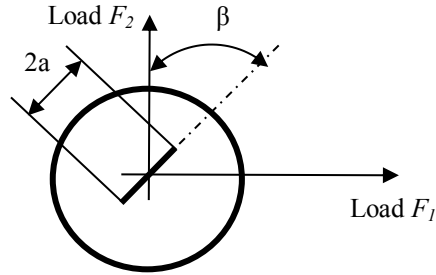


Fig. 3. Small crack modeled in the specimen center.

## 2.4. Fatigue Crack Propagation

Once the crack initiation direction is established, crack propagation can be studied. In order to achieve this goal a small crack was modeled on the specimen, Fig.3. This small crack can be used to calculate the Stress Intensity Factors (8) for the crack opening mode I and II, throughout the loading path. This step is very important because the crack will open and close as the loads on both specimen arms vary. Different initiation direction angles were considered in order to account for the different results obtained in the previous step.

$$K_{I,II} = Y_{I,II} \sigma \sqrt{\pi a} \quad (8)$$

In order to account for the Stress Intensity Factor variation throughout the cycle several authors have developed different parameters to calculate an equivalent value for the Stress Intensity Factor, taking into account both crack opening modes. The J integral (9) can be used to calculate one value to assess the fatigue crack propagation under biaxial loading.

$$J = \frac{K_I^2}{E} + \frac{K_{II}^2}{E} \quad (9)$$

Mattheij et al. developed a parameter considering that the crack propagation direction is the one that maximizes the equivalent value of (10) over the  $\beta$  angle:

$$K_{eq} = \frac{4\sqrt{2}K_{II}^3 \left( K_I + 3\sqrt{K_I^2 + 8K_{II}^2} \right)}{\left( K_I^2 + 12K_{II}^2 - K_I \sqrt{K_I^2 + 8K_{II}^2} \right)^{\frac{3}{2}}} \quad (10)$$

All these methods were used in order to predict the crack propagation direction as a function of the different non-proportional paths applied.

## 3. Numerical Calculations and Results

### 3.1. Fatigue Crack Initiation

Equations (2) to (7) were applied in order to determine the Findley, Brown and Miller, Fatemi-Socie, SWT, Liu I and Chu parameters. As critical plane methods it is also possible to determine the fatigue crack initiation direction, for each method. Fig. 4, shows the evolution of these parameters as the angle of initiation  $\beta$ , see Fig. 3, varying from  $-90^\circ$  to  $90^\circ$  for a phase shift of  $30^\circ$ .

Table 1 summarizes the obtained parameters for the phase shift loading considered in this work. All the criteria do not provide results for the in-phase load case because the shear stress that act at the specimen plane is always zero for all  $\beta$  angles. This leads that for all the criteria the parameter provided is constant, independent of  $\beta$ , or even null in the case of parameters that depend on shear.

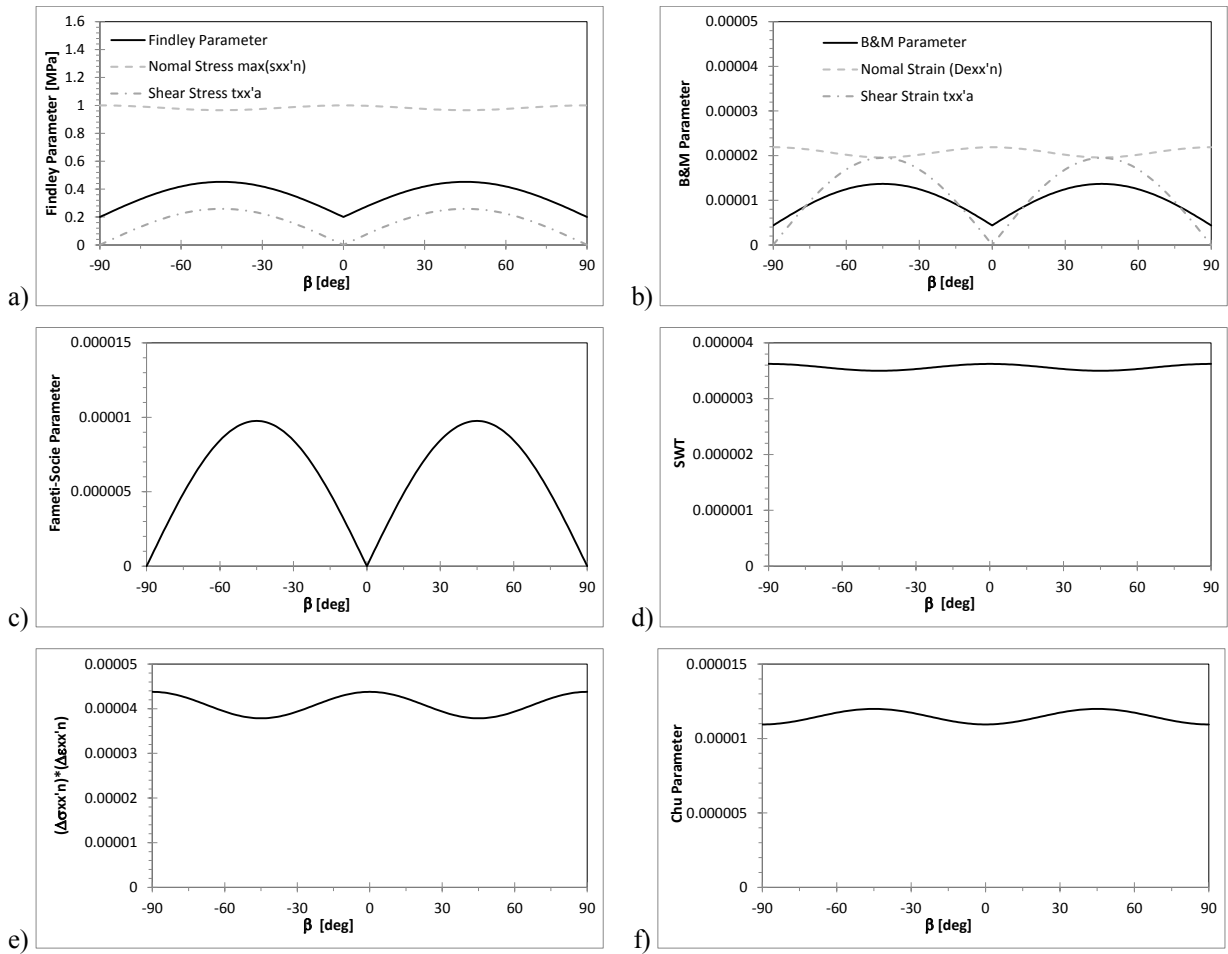


Fig. 4. Fatigue crack initiation criteria for different parameters and crack initiation angles, for a phase 30°. a) Findley, b) Brown-Miller, c) Fatemi-Socie, d) SWT, e) Liu I, f) Chu

For out-of-phase loadings it was possible to assess that loading paths have a small influence on the determined fatigue crack initiation direction angle  $\beta$ . Findley, Brown-Miller and Fatemi-Socie parameters depend also on material properties ( $k$  and  $S$ ) which were considered as  $k = 0.2$  and  $S = 0.2$ , representative of AISI303 stainless steel, Reis et al. (2009), but, a small change of these parameters only has influence on the load case with  $\delta = 180^\circ$ , which may change slightly de crack initiation angle. As one can see for the out-of-phase load cases studied the predicted fatigue initiation angle is always  $45^\circ$  for the Findley, Brown-Miller, Fatemi-Socie, Lui I, Liu II and Chu models, and  $90^\circ$  for the SWT and Liu I models.

Table 1. Fatigue crack initiation predicted angles by several criteria ( $\beta$  angle in  $[\circ]$ ).

	Findley	Brown-Miller	Fatemi-Socie	SWT	Liu I	Chu
$\delta = 0^\circ$	-	-	-	-	-	-
$\delta = 180^\circ$	-51/51	-51/51	-45/45	-90/0/90	-90/0/90	-45/45
$\delta = 30^\circ$	-45/45	-45/45	-45/45	-90/0/90	-90/0/90	-45/45
$\delta = 45^\circ$	-45/45	-45/45	-45/45	-90/0/90	-90/0/90	-45/45
$\delta = 60^\circ$	-45/45	-45/45	-45/45	-90/0/90	-90/0/90	-45/45
$\delta = 90^\circ$	-45/45	-45/45	-45/45	-90/0/90	-90/0/90	-45/45

3.2. Fatigue Crack Propagation

Using equations (9) and (10) for a fully reversed cycle (phase shift 180°) and for a 30° phase shift loading, Fig. 5 a) to f) show that the crack behaviour depends on the initial crack angle  $\beta$ . Although the individual values of  $K_I$  and  $K_{II}$  are not represented, it is clear that when the equivalent value of  $K_{eq}$  or  $J$  tends to zero, the crack is closed.

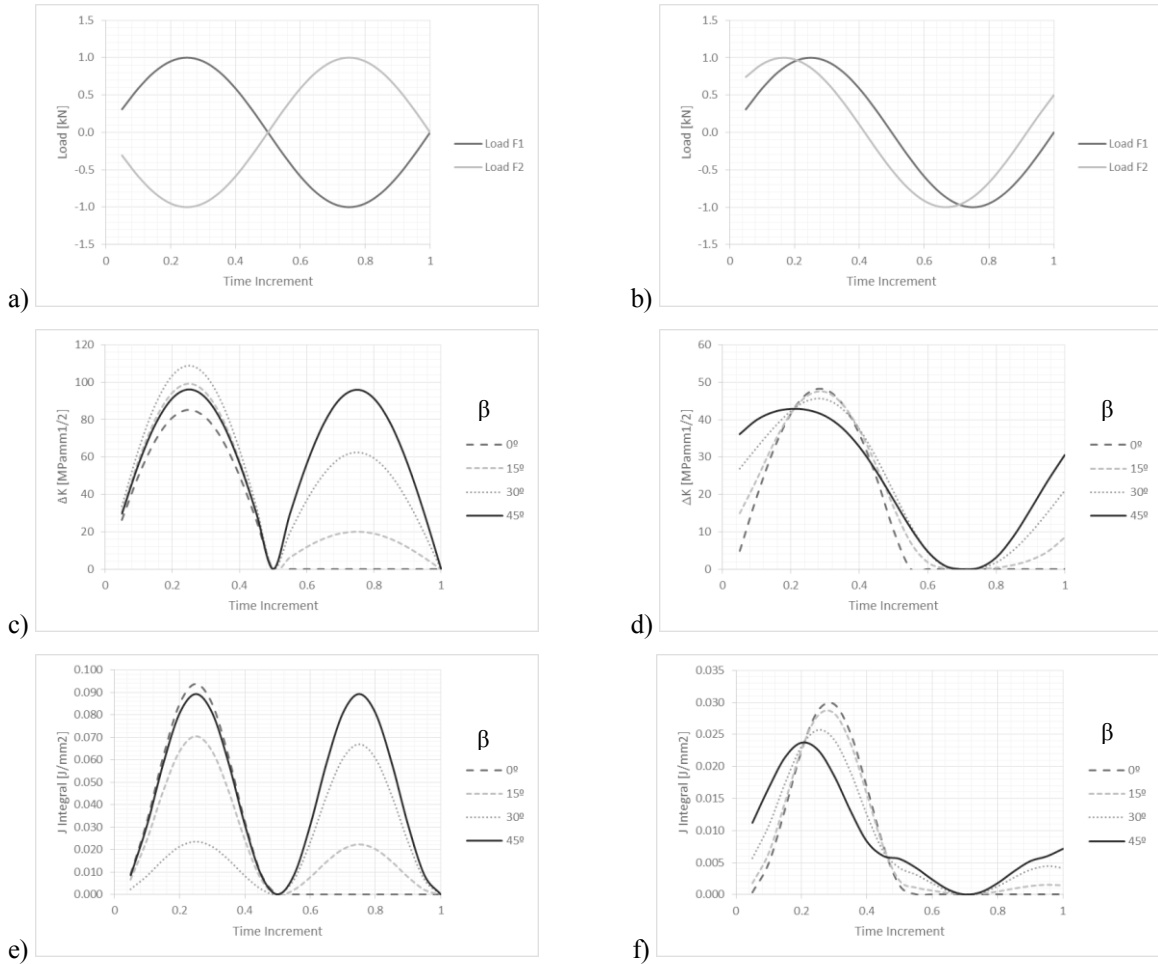


Fig. 5. Fatigue crack propagation equivalent parameters variations in one cycle. a) applied loads in a fully reversed cycle, c)  $K_{eq}$  using equation (9) for a fully reversed cycle, e)  $J$  integral for a fully reversed cycle, b) applied loads in a 30° phase shift cycle, d)  $K_{eq}$  using equation (9) in a 30° phase shift cycle, f)  $J$  integral in a 30° phase shift cycle

As one can see in Fig. 5 for a crack perpendicular to the loading direction 1 ( $\beta=0^\circ$ ), as the Load 1 reaches negative values the crack is closed, but as the  $\beta$  angle increases the crack will be open, even for negative values of Load 1.

In order to compare the influence of the out-of-phase loading path applied, the  $\Delta K_{eq} = K_{max} - K_{min}$  was calculated for all the phase shift angles considered. Table 2 summarizes the obtained results. As one can see as  $\delta$  increases  $\Delta K_{eq}$  also increases. For a 30° phase shift angle, the maximum  $\Delta K_{eq}$  occurs for a  $\beta$  angle of 0°, for a 45° phase shift angle, the maximum  $\Delta K_{eq}$  occurs for a  $\beta$  angle of 15°, for a 60°, 90° and 180° phase shift angle the maximum  $\Delta K_{eq}$  occurs for a  $\beta$  angle of 30°.

Table 2.  $\Delta K_{eq}$  Equivalent Stress Intensity Factor range [MPamm<sup>1/2</sup>] and Fatigue crack propagation angle.

$\beta$ (crack propagation angle)	$\delta=0^\circ$	$\delta=180^\circ$	$\delta=30^\circ$	$\delta=45^\circ$	$\delta=60^\circ$	$\delta=90^\circ$
0°	44.4	85.2	<b>48.0</b>	52.4	57.4	67.9
15°	44.4	99.1	47.5	<b>52.6</b>	59.1	74.1
30°	44.4	<b>108.8</b>	45.4	51.0	<b>60.3</b>	<b>78.0</b>
45°	44.4	96.1	42.9	44.9	52.9	67.7
Maximun $\beta$ angle	-	30°	0°	15°	30°	30°

Calculating the J integral range ( $\Delta J$ ), the maximum value will always occur for a  $\beta$  angle of 0° (crack perpendicular to the loading direction 1) and this value is not dependent on the non-proportional loading phase shift angle.

#### 4. Conclusions

In this paper the authors present a preliminary work to better understand the fatigue crack initiation and propagation in biaxial in-plane loadings. Using previously optimized cruciform specimen geometries, and different loading paths, a full map of principal stresses ranges was used to predict the fatigue crack initiation direction using critical plane methods. It was possible to conclude that none of the methods can predict crack initiation direction for  $\delta=0^\circ$  (in-phase loadings) and for out-of-phase loadings lead to inconsistent results between different criteria.

Finally equivalent values of J Integral and Stress Intensity Factor were calculated through the fatigue cycle, and it was verified that only the second parameter can be used to determine the fatigue crack propagation direction as a function of the non-proportional loading path.

#### References

- Babaei, S., Ghasemi-Ghalebahman, A., Hajighorbani, R., 2015. A fatigue model for sensitive materials to non-proportional loadings. *International Journal of Fatigue*, 80, pp.266–277.
- Baptista, R., Claudio, R.A., Reis, L., Madeira, J.F.A., Guelho, I., Freitas, M., 2015. Optimization of cruciform specimens for biaxial fatigue loading with direct multi search. *Theoretical and Applied Fracture Mechanics*, 80, pp.65–72.
- Cláudio, R.A., Reis, L., Freitas, M., 2014. Biaxial high-cycle fatigue life assessment of ductile aluminium cruciform specimens. , 73, pp.82–90.
- Gotoh, K., Niwa, T., Anai, Y., 2015. Numerical simulation of fatigue crack propagation under biaxial tensile loadings with phase differences. *Marine Structures*, 42, pp.53–70.
- M. Freitas, L. Reis, B. Li, I. Guelho, V. Antunes, J. Maia, R.A. Cláudio, 2013. In-plane biaxial fatigue testing machine powered by linear iron core motors. Sixth Symposium on Application of Automation Technology in Fatigue and Fracture Testing and Analysis, ASTM STP 1571, pp. 63-79.
- Misak, H.E., Perel, V.Y., Sabelkin, V., S. Mall 2014. Biaxial tension–tension fatigue crack growth behavior of 2024-T3 under ambient air and salt water environments. *Engineering Fracture Mechanics*, 118, pp.83–97.
- Misak, H.E., Perel, V.Y., Sabelkin, V., S. Mall, 2013. Corrosion fatigue crack growth behavior of 7075-T6 under biaxial tension–tension cyclic loading condition. *Engineering Fracture Mechanics*, 106, pp.38–48.
- Misak, H.E., Perel, V.Y., Sabelkin, V., S. Mall, 2013. Crack growth behavior of 7075-T6 under biaxial tension-tension fatigue. *International Journal of Fatigue*, 55, pp.158–165.
- Misra, A., Singh, V.K., Scholar, M.T., 2007. Prediction of Crack Initiation Direction and Fatigue and Crack Growth Under Mixed Mode Loading. SEM Annual Conference & Exposition on Experimental and Applied Mechanics.
- Plank, R., Kuhn, G., 1999. Fatigue crack propagation under non-proportional mixed mode loading. *Engineering Fracture Mechanics*, 62(2-3), pp.203–229.
- Reis, L, Li, B. Freitas, M. (2009). Crack initiation and growth path under multiaxial fatigue loading in structural steels. *International Journal of Fatigue*. Volume 31, Issues 11-12, pp 1660-1668.
- Socie, D.F., Marquis, G.B., (2000) Multiaxial fatigue, SAE International.
- Zerres, P., Vormwald, M., 2014. Review of fatigue crack growth under non-proportional mixed-mode loading. *International Journal of Fatigue*, 58, pp.75–83..